PERGAMON

International Journal of Solids and Structures 37 (2000) 5203–5217

INTERNATIONAL JOURNAL OF SOLIDS and STRUCTURES

www.elsevier.com/locate/ijsolstr

Flexible translational joint analysis by meshless method

M. Iura*, J. Kanaizuka

Department of Civil Engineering, Tokyo Denki University, Hatoyama, Hiki, Saitama, Japan

Received 20 May 1999; in revised form 15 July 1999

Abstract

Element free Galerkin method (EFGM) is used to analyze a flexible translational joint. A moving constraint condition is a major concern for the translational joint analysis. It is shown that the EFGM is well suited for an analysis of flexible translational joint. Original shape function in the EFGM is modified so that essential boundary conditions are imposed by the same way as that of finite element method (FEM). The modified shape function possesses physical values at both ends of the element. The completeness of the modified shape function is discussed. Employing the present modified shape function makes easy to implement the moving constraint condition. Numerical examples for a static cantilever beam are presented for a comparison between the penalty method, the Lagrange multiplier method and the present one. As second example, a large deformation problem is solved for a comparison between the FEM and the EFGM. Finally, a simulation of flexible translational joint is shown. © 2000 Elsevier Science Ltd. All rights reserved.

Keywords: Meshless; Beam; Dynamics; Multibody; Nonlinear

1. Introduction

In this paper, we consider a flexible translational joint as shown in Fig. 1. This system is modeled by two flexible beams. Point B slides along the beam N and point D along a rigid ground. When the bodies of translational joint are assumed to be rigid, a moving constraint condition of translational joint takes a simple form (see, for example, Haug, 1989). In spite of potential demand for using flexible bodies, very few studies have been done on flexible translational joint analysis. The translational joint mechanism becomes a slider-crank mechanism when point B does not slide along the beam N. In such a case or flexible multibody dynamics, the finite element method (FEM) has been used (Cardona and Geradin, 1991; Escalona et al., 1998; Iura and Atluri, 1995; Simo and Vu-Quoc, 1986). When the FEM

* Corresponding author. Fax: +81-492-96-6501.
E-mail address: iura@g.dendai.ac.jp (M. Iura).

0020-7683/00/$ - see front matter © 2000 Elsevier Science Ltd. All rights reserved.
PII: S0020-7683(99)00208-5

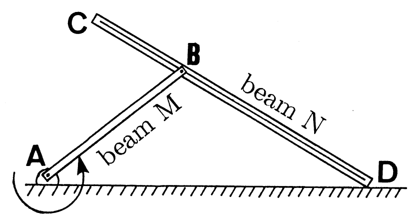

Fig. 1. Flexible translational joint.

is used for a simulation of flexible translational joint, we might employ a finite element model as shown in Fig. 2. The moving constraint condition asserts that point B of the beam M should lie on the i–j element of the beam N. Once point B passes the node j, the constraint condition implies that point B should lie on the j–k element of the beam N. A difficulty in the finite element analysis is to obtain an exact time when point B passes the node j. Even if very fine time increments are used for a simulation, it might be difficult to obtain the exact passing time. When a meshless method is employed for a flexible translational joint analysis, a displacement at an arbitrary point in the meshless element is presented by just inserting position coordinates into a shape function. It is unnecessary to obtain the exact time when point B passes the node j. Therefore, a constant time increment is available throughout a simulation. This fact shows that the meshless method is well suited for satisfying the moving constraint condition.

In meshless methods, there exist a variety of formulation, such as diffuse element method (Nayroles et al., 1992), EFGM (Belytschko et al., 1994), reproducing kernel particle method (Liu et al., 1995), hp-clouds method (Duarte and Oden, 1996), meshless local Petrov–Galerkin method (Atluri and Zhu, 1998), finite point method (Onate et al., 1996) and partition of unity (Melenk and Babuska, 1996). Among the existing meshless methods, a difficulty is encountered in imposing essential boundary conditions. This difficulty comes from the property of an approximation $u^h(x)$ for $u(x)$, expressed as

$$u^h(x_i) = \sum_j N_j(x_i) u_j \neq u_i. \tag{1}$$

For satisfying $u(x_i) = 0$, it is not sufficient to impose $u_i = 0$ at $x = x_i$. Therefore, u_i is called the nodal value at $x = x_i$. A variety of techniques have been proposed for satisfying essential boundary conditions (Gunther and Liu, 1998; Kaljevic and Saigal, 1997; Krongauz and Belytschko, 1996; Lu et al., 1994; Modaressi and Aubert, 1996). The existing methods for imposing essential boundary conditions are more complicated than that of the FEM. It will be very effective to find a meshless method in which essential boundary conditions are imposed by the same way as that of the FEM.

After giving a brief explanation of the EFGM in Section 2, we propose a modified shape function in Section 3. The idea is to introduce a variable defined by

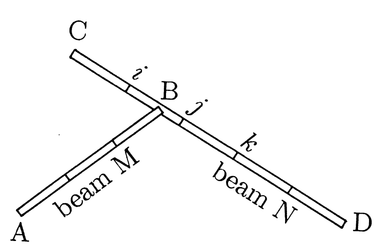

Fig. 2. Finite element model for translational joint.

$$U_i = u^h(x_i) = \sum_j N_j(x_i)u_j. \tag{2}$$

The variable U_i denotes the physical value at $x = x_i$ by the definition. The nodal value u_i is replaced by the variable U_i in the modified approximation. It is sufficient, therefore, for satisfying $u(x_i) = 0$ to impose $U_i = 0$ at $x = x_i$. This fact implies that we can impose the essential boundary conditions by the same way as that of the FEM. Since the resulting shape function differs from the original shape function, we discuss the reproducing condition or completeness of the modified shape function in Section 3.

In multibody dynamics, a treatment of constraint conditions is a major concern. Joint constraints appear in translational joint mechanism. In Section 4, using the joint constraints, we eliminate dependent variables from the displacement functions. Equations of motion for the translational joint mechanism are presented in Section 5 with the aid of Hamilton's principle. Numerical examples are given in Section 6.

2. Element free Galerkin method

Based on the work of Belytschko et al. (1994), we briefly summarize the EFGM. The approximation u^h of a function $u(x)$ is expressed as

$$u^h(\boldsymbol{x}) = \sum_j^m p_j(\boldsymbol{x})a_j(\boldsymbol{x}) \equiv p^{\mathrm{T}}(\boldsymbol{x})\boldsymbol{a}(\boldsymbol{x}), \tag{3}$$

where $p_j(\boldsymbol{x})$ are basis functions, $a_j(\boldsymbol{x})$ are their coefficients and m is the number of terms in the basis. An example of polynomial basis is written as

$$\boldsymbol{p}^{\mathrm{T}}(\boldsymbol{x}) = \left[1, x, x^2\right] \quad (m = 3). \tag{4}$$

The coefficients $a_j(\boldsymbol{x})$ are obtained by minimizing the following function J:

$$J = \frac{1}{2}\sum_i^n w(\boldsymbol{x} - \boldsymbol{x}_i)\left[\boldsymbol{p}^{\mathrm{T}}(\boldsymbol{x}_i)\boldsymbol{a}(\boldsymbol{x}) - u_i\right]^2, \tag{5}$$

where n is the number of points in the neighborhood of $\boldsymbol{x}$ for which a weighting function $w(\boldsymbol{x} - \boldsymbol{x}_i) \neq 0$, and u_i is the nodal value of u at $\boldsymbol{x} = \boldsymbol{x}_i$. The stationary of J in Eq. (5) with respect to $\boldsymbol{a}(\boldsymbol{x})$ leads to

$$\boldsymbol{a}(\boldsymbol{x}) = \boldsymbol{A}^{-1}(\boldsymbol{x})\boldsymbol{B}(\boldsymbol{x})\boldsymbol{u}, \tag{6}$$

where

$$\boldsymbol{A}(\boldsymbol{x}) = \sum_i^n w(\boldsymbol{x} - \boldsymbol{x}_i)\boldsymbol{p}(\boldsymbol{x}_i)\boldsymbol{p}^{\mathrm{T}}(\boldsymbol{x}_i), \tag{7}$$

$$\boldsymbol{B}(\boldsymbol{x}) = \left[w(\boldsymbol{x} - \boldsymbol{x}_1)\boldsymbol{p}(\boldsymbol{x}_1), w(\boldsymbol{x} - \boldsymbol{x}_2)\boldsymbol{p}(\boldsymbol{x}_2), \ldots, w(\boldsymbol{x} - \boldsymbol{x}_n)\boldsymbol{p}(\boldsymbol{x}_n)\right], \tag{8}$$

$$\boldsymbol{u}^{\mathrm{T}} = [u_1, u_2, \ldots, u_n]. \tag{9}$$

Note that u_j does not denote the physical value at $\boldsymbol{x}_j$. Therefore, a variety of methods have been proposed for imposing essential boundary conditions.

Substitution of Eq. (6) into Eq. (3) leads to

$$u^h(\boldsymbol{x}) = \boldsymbol{p}^{\mathrm{T}}(\boldsymbol{x})\boldsymbol{A}^{-1}(\boldsymbol{x})\boldsymbol{B}(\boldsymbol{x})\boldsymbol{u} \equiv \boldsymbol{N}(\boldsymbol{x})\boldsymbol{u}, \tag{10}$$

where the shape function $\boldsymbol{N}(\boldsymbol{x})$ is written as

$$\boldsymbol{N}(\boldsymbol{x}) = \boldsymbol{p}^{\mathrm{T}}(\boldsymbol{x})\boldsymbol{A}^{-1}(\boldsymbol{x})\boldsymbol{B}(\boldsymbol{x}). \tag{11}$$

A weighting function has been defined in terms of polynomial or exponential functions (Belytschko et al., 1996). In this paper, the following weighting function is used:

$$w(d_i) = \begin{cases} 1 - 6\left(\dfrac{d_i}{r}\right)^2 + 8\left(\dfrac{d_i}{r}\right)^3 - 3\left(\dfrac{d_i}{r}\right)^4 & (d_i \le r), \\ 0 & (d_i \ge r), \end{cases} \tag{12}$$

where d_i is defined as $d_i = \|\boldsymbol{x} - \boldsymbol{x}_i\|$, and r is the radius of the support for the weight function.

3. A modified shape function

As described before, a difficulty in the meshless method is encountered in imposing essential boundary conditions. In the case of flexible translational joint analysis, the essential boundary conditions are imposed on the ends of beam. If a displacement function has physical values at the ends of beam, it might be easy to satisfy the essential boundary conditions. In this paper, we propose a modified shape function in which both ends of beam possess physical values in stead of nodal values.

Let x_1 and x_n denote the coordinates at both ends of the element. The physical values at x_1 and x_n are denoted by U_1 and U_n respectively. Then, by the definition, we have

$$\begin{aligned} N_1(x_1)u_1 + \cdots + N_n(x_1)u_n &= U_1, \\ N_1(x_n)u_1 + \cdots + N_n(x_n)u_n &= U_n. \end{aligned} \tag{13}$$

Solving Eq. (13) for u_1 and u_n, we have

$$\begin{pmatrix} u_1 \\ u_n \end{pmatrix} = \begin{pmatrix} N_1(x_1) & N_n(x_1) \\ N_1(x_n) & N_n(x_n) \end{pmatrix}^{-1} \begin{pmatrix} p_1(x_1) \\ p_n(x_n) \end{pmatrix}, \tag{14}$$

where $p_1(x_1)$ and $p_n(x_n)$ are written as

$$\begin{aligned} p_1(x_1) &= U_1 - \left\{N_2(x_1)u_2 + \cdots + N_{n-1}(x_1)u_{n-1}\right\}, \\ p_n(x_n) &= U_n - \left\{N_2(x_n)u_2 + \cdots + N_{n-1}(x_n)u_{n-1}\right\}. \end{aligned} \tag{15}$$

Substitution of Eq. (14) into Eq. (10) leads to

$$u^h(\boldsymbol{x}) = \boldsymbol{N}^*(\boldsymbol{x})\boldsymbol{u}^*, \quad \boldsymbol{u}^* = [U_1, u_2, \ldots, u_{n-1}, U_n]. \tag{16}$$

The modified shape function $\boldsymbol{N}^* = [N_1^*, \ldots, N_n^*]^{\mathrm{T}}$ is expressed by

$$N_1^*(x) = \left\{N_n(x_n)N_1(x) - N_1(x_n)N_n(x)\right\}/W^*,$$

$$N_j^*(x) = N_j + M_j(x), \quad (j = 2, \ldots, n-1),$$

$$N_n^*(x) = \{N_1(x_1)N_n(x) - N_n(x_1)N_1(x)\}/W^*, \tag{17}$$

where M_j and W^* are defined as

$$M_j = \frac{1}{W^*}\left[N_1(x)\{N_n(x_1)N_j(x_n) - N_n(x_n)N_j(x_1)\} + N_n(x)\{N_1(x_n)N_j(x_1) - N_1(x_1)N_j(x_n)\}\right], \tag{18}$$

$$W^* = N_1(x_1)N_n(x_n) - N_1(x_n)N_n(x_1). \tag{19}$$

Since the modified shape function is different from the original one, a question about consistency might be raised. Consistency conditions are closely related to the reproducing conditions or completeness (Belytschko et al., 1996, 1998). In what follows, we shall discuss the reproducing conditions.

According to Belytschko et al. (1998), the original shape function of the EFGM satisfies the reproducing conditions, expressed as

$$\sum_{i=1}^{n} N_i(x)x_i^k = x^k, \quad (k = 1, 2, \ldots). \tag{20}$$

Since Eq. (20) holds at $x = x_1$ and $x = x_n$, we have

$$\sum_{j=2}^{n-1} N_j(x_1)x_j^k = x_1^k - N_1(x_1)x_1^k - N_n(x_1)x_n^k,$$

$$\sum_{j=2}^{n-1} N_j(x_n)x_j^k = x_n^k - N_1(x_n)x_1^k - N_n(x_n)x_n^k. \tag{21}$$

Using Eqs. (17)–(21), we have the relationship expressed as

$$N_1^*(x)x_1^k + N_n^*(x)x_n^k + \sum_{j=2}^{n-1} M_j(x)x_j^k = N_1(x)x_1^k + N_n(x)x_n^k. \tag{22}$$

To show the reproducing condition of the modified shape function, we utilize Eq. (17) in the following equation:

$$\sum_{i=1}^{n} N_i^*(x)x_i^k = \sum_{j=2}^{n-1} N_j^*(x)x_j^k + N_1^*(x)x_1^k + N_n^*(x)x_n^k$$

$$= \sum_{j=1}^{n} N_j(x)x_j^k - N_1(x)x_1^k - N_n(x)x_n^k + N_1^*(x)x_1^k + N_n^*(x)x_n^k + \sum_{j=2}^{n-1} M_j(x)x_j^k. \tag{23}$$

Substituting Eq. (22) into Eq. (23) and using Eq. (20), we obtain

$$\sum_{i=1}^{n} N_i^*(x) x_i^k = \sum_{j=1}^{n} N_j(x) x_j^k = x^k. \tag{24}$$

The above equation shows that the reproducing condition of the present shape function is met.

It should be noted that boundary conditions are not always prescribed at both ends of the element. When boundary conditions are prescribed at $x = x_k$ except the ends of the element, we should introduce the physical value at $x = x_k$. The way for deriving the displacement function with the physical value at $x = x_k$ is exactly the same as that described above.

4. Flexible translational joint

It is a crucial point in multibody dynamic analysis to satisfy constraint conditions. The Lagrange multiplier method has been introduced to account for the effect of kinematic constraints (see, for example, Haug, 1989). This method leads to a mixed system of differential algebraic equations. Another method for satisfying constraint conditions is to eliminate the dependent variables from the basic equations, so that the resulting equations of motion are ordinary differential equations (ODEs). It is not always possible to eliminate the dependent variables from the equations of motion. If the elimination is accomplished, however, a well established integration scheme is available for integrating the ODEs. In this paper, we eliminate the dependent variables from the equations of motion by using constraint conditions. Therefore, the constraint conditions are always satisfied.

Let us consider a flexible translational joint as shown in Fig. 3. We assume that point B of the beam M slides along the beam axis of beam N without any frictions, and that the rotation at point B of the beam M is not restricted. The convected coordinates along undeformed beams M and N are denoted by x^M and x^N, respectively. Let $\boldsymbol{d}^M$ and $\boldsymbol{d}^N$ denote the displacement vectors at the beam axes associated with the beams M and N, respectively. Then, the displacement vectors at the beam axes are expressed as

$$\boldsymbol{d}^M = \left(\sum_{i=1}^{l} N_i^*(x^M) u_i^M \right) \boldsymbol{e}_1^M + \left(\sum_{i=1}^{l} N_i^*(x^M) v_i^M \right) \boldsymbol{e}_2^M,$$

$$\boldsymbol{d}^N = \left(\sum_{i=1}^{s} N_i^*(x^N) u_i^N \right) \boldsymbol{e}_1^N + \left(\sum_{i=1}^{s} N_i^*(x^N) v_i^N \right) \boldsymbol{e}_2^N, \tag{25}$$

where $\boldsymbol{e}_\alpha^M$ and $\boldsymbol{e}_\alpha^N$ are the base vectors associated with the beams M and N, respectively, as shown in Fig. 3. The notations u_i^M and v_i^M are nodal values associated with the base vectors $\boldsymbol{e}_1^M$ and $\boldsymbol{e}_2^M$,

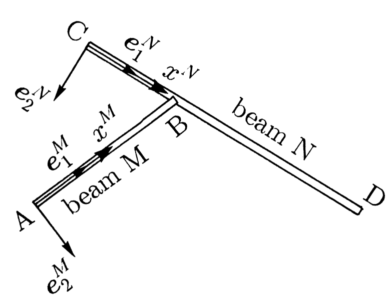

Fig. 3. Base vectors and coordinate systems for translational joint.

respectively, and u_i^N and v_i^N nodal values associated with the base vectors $\boldsymbol{e}_1^N$ and $\boldsymbol{e}_2^N$, respectively. The notations l and s denote the number of nodes for the beams M and N, respectively. It should be noted that u_1^M, v_1^M, u_l^M, v_l^M, u_1^N, v_1^N, u_s^N and v_s^N are the physical values or the displacement components at each node.

Let x_B^N be the coordinate of point B along the beam N at time $t = 0$ as shown in Fig. 4, in which the dotted lines denote the initial configuration and the solid lines the deformed one. At time $t = T$, the coordinate of point B along the beam N may be denoted by $x_B^N + \xi_B$, where ξ_B is a variable. The constraint condition such that point B of the beam M should lie on the beam N may be written as

$$\boldsymbol{d}_B^M = \xi_B \boldsymbol{e}_1^N + \boldsymbol{d}_B^N, \tag{26}$$

where the displacement vectors $\boldsymbol{d}_B^M$ and $\boldsymbol{d}_B^N$ are expressed in terms of components by

$$\boldsymbol{d}_B^M = \left(\sum_{i=1}^{l} N_i^*\left(x_B^M\right)u_i^M\right)\boldsymbol{e}_1^M + \left(\sum_{i=1}^{l} N_i^*\left(x_B^M\right)v_i^M\right)\boldsymbol{e}_2^M, \tag{27}$$

$$\boldsymbol{d}_B^N = \left(\sum_{i=1}^{s} N_i^*\left(x_B^N + \xi_B\right)u_i^N\right)\boldsymbol{e}_1^N + \left(\sum_{i=1}^{s} N_i^*\left(x_B^N + \xi_B\right)v_i^N\right)\boldsymbol{e}_2^N, \tag{28}$$

where x_B^M is the initial coordinate of point B along the beam M.

At initial state as shown in Fig. 3, the relationships between the base vectors $\boldsymbol{e}_\alpha^M$ and $\boldsymbol{e}_\alpha^N$ are written as

$$\begin{Bmatrix} \boldsymbol{e}_1^M \\ \boldsymbol{e}_2^M \end{Bmatrix} = \begin{pmatrix} \cos\alpha & -\sin\alpha \\ \sin\alpha & \cos\alpha \end{pmatrix} \begin{Bmatrix} \boldsymbol{e}_1^N \\ \boldsymbol{e}_2^N \end{Bmatrix}. \tag{29}$$

By substituting Eqs. (27)–(29) into Eq. (26), we have the following relationships:

$$\left(\sum_{i=1}^{l} N_i^*\left(x_B^M\right)u_i^M\right)\cos\alpha + \left(\sum_{i=1}^{l} N_i^*\left(x_B^M\right)v_i^M\right)\sin\alpha = \xi_B + \sum_{i=1}^{s} N_i^*\left(x_B^N + \xi_B\right)u_i^N,$$

$$-\left(\sum_{i=1}^{l} N_i^*\left(x_B^M\right)u_i^M\right)\sin\alpha + \left(\sum_{i=1}^{l} N_i^*\left(x_B^M\right)v_i^M\right)\cos\alpha = \sum_{i=1}^{s} N_i^*\left(x_B^N + \xi_B\right)v_i^N. \tag{30}$$

Since the present displacement function possesses the physical values at both ends of beam, we have $u_l^M = u_B^M$ and $v_l^M = v_B^M$.

Solving Eq. (30) for u_B^M and v_B^M leads to

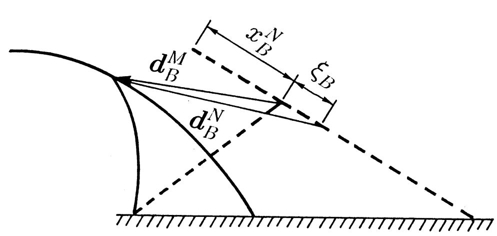

Fig. 4. Initial and deformed configurations for translational joint.

$$u_B^M = \frac{1}{N_l^*(x_B^M)}\left[\xi_B \cos\alpha - \sum_{i=1}^{l-1} N_i^*(x_B^M)u_i^M + \sum_{i=1}^{s} N_i^*(x_B^N + \xi_B)u_i^N \cos\alpha - \sum_{i=1}^{s} N_i^*(x_B^N + \xi_B)v_i^N \sin\alpha\right], \quad (31)$$

$$v_B^M = \frac{1}{N_l^*(x_B^M)}\left[\xi_B \sin\alpha - \sum_{i=1}^{l-1} N_i^*(x_B^M)v_i^M + \sum_{i=1}^{s} N_i^*(x_B^N + \xi_B)v_i^N \cos\alpha + \sum_{i=1}^{s} N_i^*(x_B^N + \xi_B)u_i^N \sin\alpha\right]. \quad (32)$$

The above equations show that the displacement components u_B^M and v_B^M are expressed in terms of ξ_B and the nodal values of the beams M and N. The constraint condition, expressed by Eq. (26), is satisfied by eliminating u_B^M and v_B^M from the displacement functions. Introducing Eqs. (31) and (32) into the displacement functions of the beam M, we obtain the following expression:

$$u^M = \sum_{i=1}^{l-1} N_i^*(x^M)u_i^M + N_l^*(x^M)u_l^M,$$

$$= \sum_{i=1}^{l-1} A_i u_i^M + \sum_{i=1}^{n} B_i\left(u_i^N \cos\alpha - v_i^N \sin\alpha\right) + \frac{N_l^*(x^M)}{N_l^*(x_B^M)}\xi_B \cos\alpha, \quad (33)$$

$$v^M = \sum_{i=1}^{l-1} N_i^*(x^M)v_i^M + N_l^*(x^M)v_l^M,$$

$$= \sum_{i=1}^{l-1} A_i v_i^M + \sum_{i=1}^{n} B_i\left(v_i^N \cos\alpha + u_i^N \sin\alpha\right) + \frac{N_l^*(x^M)}{N_l^*(x_B^M)}\xi_B \sin\alpha, \quad (34)$$

where

$$A_i = N_i^*(x^M) - \frac{N_l^*(x^M)}{N_l^*(x_B^M)}N_i^*(x_B^M),$$

$$B_i = \frac{N_l^*(x^M)}{N_l^*(x_B^M)}N_i^*(x_B^N + \xi_B). \quad (35)$$

In Timoshenko's beam theory, independent variables are translational and rotational ones. The displacement function for the rotation of the beam M remains unchanged since the rotation at point B of the beam M is not restricted. The displacement functions for the beam N remain also unchanged. Therefore, the displacement functions for the rotation ϕ^M and those for the beam N are expressed as

$$\phi^M = \sum_{i=1}^{l} N_i^*(x^M)\phi_i^M,$$

$$u^N = \sum_{i=1}^{s} N_i^*(x^N)u_i^N,$$

$$v^N = \sum_{i=1}^{s} N_i^*(x^N) v_i^N,$$

$$\phi^N = \sum_{i=1}^{s} N_i^*(x^N) \phi_i^N. \tag{36}$$

5. Formulation

In this paper, we assume that there exists no damping forces. Then, the equations of motion for the present system are derived with the help of Hamilton's principle which states that

$$\delta H = 0,$$

$$H = \int_{t1}^{t2} [T - \Pi_s - \Pi_f] \, dt, \tag{37}$$

where H denotes the total potential energy, T the kinetic energy, Π_s the strain energy and Π_f the potential energy of external forces. According to Iura and Atluri (1988, 1995 and Reissner, 1981), the kinetic energy and the strain energy for Timoshenko's beam are expressed as

$$T = \int_{t1}^{t2} \frac{1}{2} \left[A_\rho(\dot{u})^2 + A_\rho(\dot{v})^2 + I_\rho(\dot{\phi})^2 \right] dt, \tag{38}$$

$$\Pi_s = \int_0^L \left[\frac{EA}{2}(\epsilon)^2 + \frac{EI}{2}(\kappa)^2 + \frac{GA_s}{2}(\gamma)^2 \right] dx, \tag{39}$$

where

$$A_\rho = \int m \, dA, \quad I_\rho = \int m y^2 \, dA, \tag{40}$$

and m is the mass density per unit volume, ϵ the axial strain, κ the curvature, γ the shearing strain, EA the stretch rigidity, EI the bending rigidity, GA_s the shearing rigidity and L the undeformed beam length. The relationships between displacements and strains are written as (Iura and Atluri, 1988, 1989)

$$\epsilon = (u' + \cos\phi_0)\cos\phi + (v' + \sin\phi_0)\sin\phi - 1,$$

$$\kappa = \phi',$$

$$\gamma = (v' + \sin\phi_0)\cos\phi - (u' + \cos\phi_0)\sin\phi, \tag{41}$$

where $(\,)' = d(\,)/dx$, and ϕ_0 is the initial angle between the beam axis and the coordinate axis. It should be noted that the above basic equations for Timoshenko's beam have been derived on the basis of a geometrically exact beam theory.

By substituting the displacement functions into Eq. (41) and using Eqs. (37)–(39), we have the following discretized equations of motion:

$$[\boldsymbol{M}]\{\ddot{\boldsymbol{D}}\} + [\boldsymbol{C}(\boldsymbol{D})]\{\dot{\boldsymbol{D}}\} + \{\boldsymbol{K}(\boldsymbol{D})\} = \{\boldsymbol{f}\}, \tag{42}$$

where $[\boldsymbol{M}]$ is the mass matrix,$[\boldsymbol{C}(\boldsymbol{D})]\{\dot{\boldsymbol{D}}\}$ and $\{\boldsymbol{K}(\boldsymbol{D})\}$ are the internal force vectors and $\{\boldsymbol{f}\}$ is the external force vector, and

$$\{\boldsymbol{D}\} = \left\{u_1^M, v_1^M, \phi_1^M, \ldots, u_{l-1}^M, v_{l-1}^M, \phi_{l-1}^M, \phi_l^M, \xi_B, u_1^N, v_1^N, \phi_1^N, \ldots, u_s^N, v_s^N, \phi_s^N\right\}^{\mathrm{T}}. \tag{43}$$

With the introduction of new variable $\mathbf{Z}$, Eq. (42) is transformed into simultaneous first-order ODE, expressed as

$$\{\dot{\boldsymbol{D}}\} = \{\boldsymbol{Z}\},$$

$$[\boldsymbol{M}]\{\dot{\boldsymbol{Z}}\} = \{\boldsymbol{f}\} - [\boldsymbol{C}(\boldsymbol{D})]\{\boldsymbol{Z}\} - \{\boldsymbol{K}(\boldsymbol{D})\}. \tag{44}$$

It should be noted that the mass matrix $[\boldsymbol{M}]$ is a constant matrix. It is enough, therefore, for each problem to calculate $[\boldsymbol{M}]^{-1}$ only once and store those values in a memory disk. At each time step, $[\boldsymbol{M}]^{-1}$ is recovered from the memory disk.

The above ODEs are integrated by the fourth-order Runge–Kutta method under boundary and initial conditions. The way for imposing essential boundary conditions is exactly the same as that of the FEM.

6. Numerical examples

In this chapter, we consider three problems. First problem is a linear static cantilever beam, in which the penalty method, the Lagrange multiplier method and the present method are used for imposing essential boundary conditions. Second problem is the flying spaghetti problem (Simo and Vu-Quoc, 1986), where the present result is compared with those obtained by the FEM. Last problem is a flexible translational joint.

Throughout the present examples in the EFGM, we employ the linear basis function expressed as

$$\boldsymbol{p}^{\mathrm{T}}(x) = [1, x]. \tag{45}$$

A weighting function used herein is expressed by Eq. (12).

6.1. Cantilever beam

We consider a cantilever beam subjected to a uniformly distributed load $p = 1$ (see Fig. 5). The following parameters are used for the present problem: Young's modulus $E = 2 \times 10^6$; shearing modulus

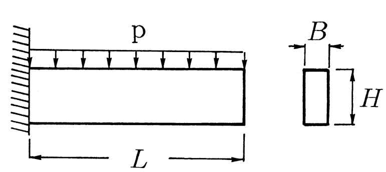

Fig. 5. Cantilever beam.

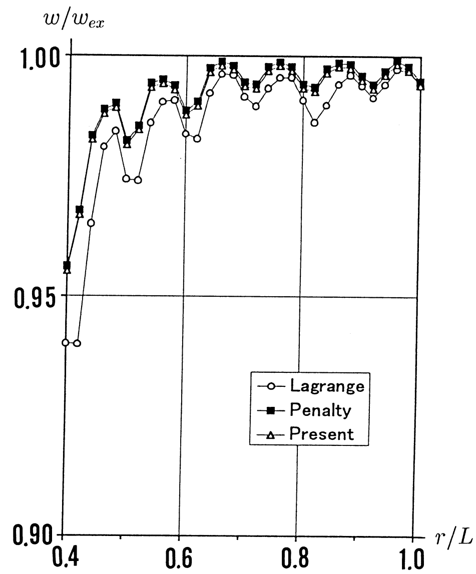

Fig. 6. Tip displacements of cantilever beam.

$G = 1 \times 10^6$; beam length $L = 1000$; width $B = 1.2$; height $H = 10$; modified area $A_s = A = 12$. The number of nodes and cells used are 11 and 10, respectively. Regular meshes for nodes and cells are used. Three-point Gauss integration rule is used for each cell. When the penalty method and the Lagrange multiplier method are used for imposing essential boundary conditions, we use the shape function defined by Eq. (10). The displacements w at the free end of the beam are shown in Fig. 6. The abscissa is taken as the ratio r/L where r is the radius of the support. The ordinate shows the ratio w/w_{ex} where w_{ex} is the exact solution of Bernoulli–Euler's beam theory. As shown in Fig. 6, the numerical solutions obtained converge with increased ratio r/L. The penalty method and the present one give almost same numerical results. The Lagrange multiplier method leads to the poor numerical results compared with other two methods.

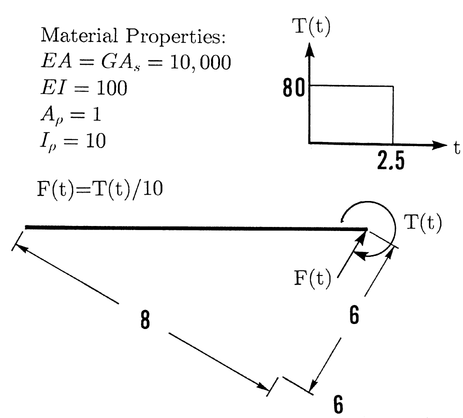

Fig. 7. Problem data for flying spaghetti.

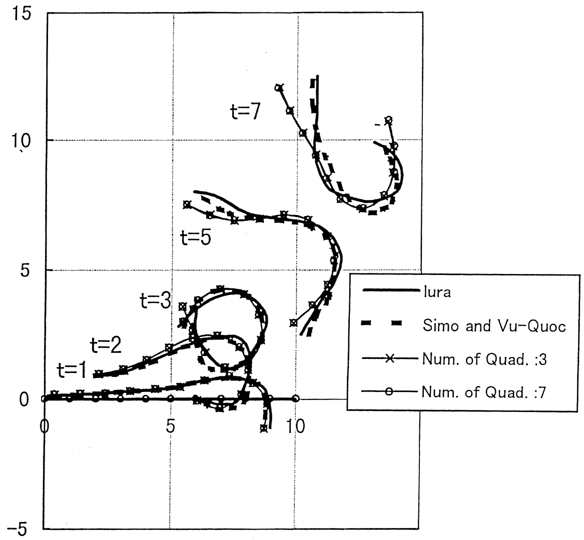

Fig. 8. Sequence of beam motion.

6.2. Flying spaghetti problem

This problem has been solved first by Simo and Vu-Quoc (1986) and later by Iura and Atluri (1988), in which the FEM has been used. The beam is subjected to force and torque applied simultaneously at one end of the beam. The problem data are given in Fig. 7. The number of nodes and cells in the EFGM are 11 and 10, respectively. Regular meshes for nodes and cells are used. The radius of the support r is 5. Three-point and seven-point Gauss integration rules are used for each cell. Time increment Δt for the integration scheme is 0.001. The sequence of the beam motion is illustrated in Fig. 8, where numerical results obtained by the FEM and the EFGM are shown. In this example, there exists no significant differences in numerical results between three-point and seven-point Gauss integration rules. A good agreement between the present results and the FEM results has been obtained.

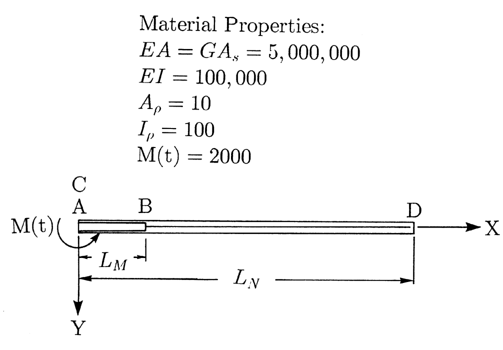

Fig. 9. Problem data for translational joint.

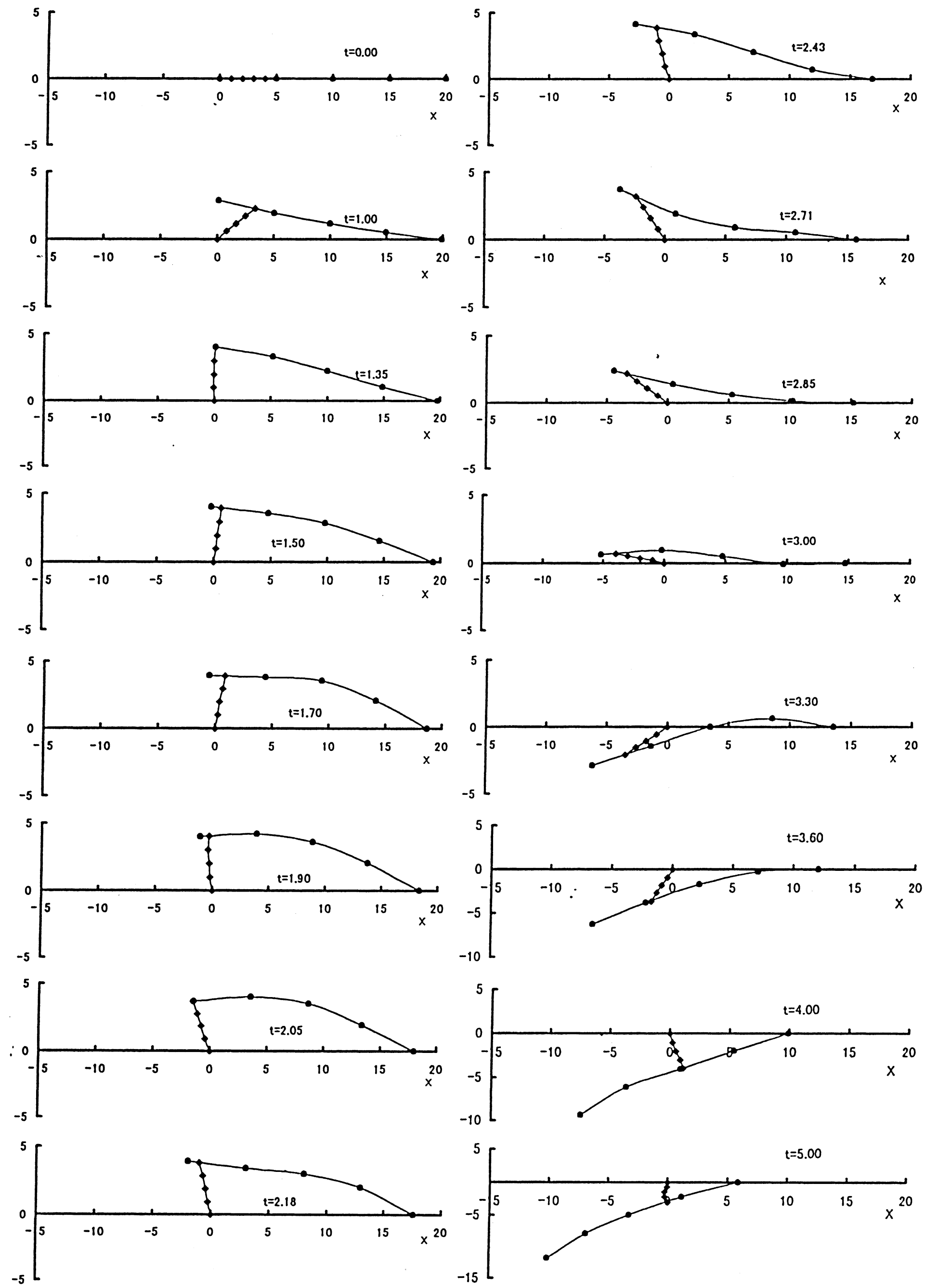

Fig. 10. Sequence of motion for flexible translational joint.

6.3. Flexible translational joint

Let us consider a flexible translational joint as shown in Fig. 9. In this mechanism, we assume that no friction forces exist. Therefore, point B and point D slide along the beam N and a rigid ground, respectively, without any frictions. The problem data are shown in Fig. 9. A torque is applied at point A of the beam M continuously. The number of nodes in the beam M and the beam N are 5 and 9, respectively. The number of cells in the beam M and the beam N are 4 and 8, respectively. Regular meshes for nodes and cells are used for each beam. The radius of the support r for the beam M and the beam N are 2 and 10, respectively. Three-point Gauss integration rules is used for each cell. Time increment Δt for the integration scheme is 0.001.

When point B approaches one end of the beam N, a contact will occur between point B and the beam N. In this paper, when a distance between point B and one end of the beam N is less than $L_N/20{,}000$, an elastic spring is inserted in the end of the beam N. A spring constant k is assumed to be 1×10^9. We confirmed that no distinct differences in numerical results were observed when a spring constant k was taken from 1×10^8 to 1×10^{11}.

The following boundary conditions are used in this system:

$$u^M = v^M = 0 \quad \text{at } x_M = 0 \quad (\text{Point } A)$$

$$v^N = 0 \quad \text{at } x_N = L_N \quad (\text{Point } D)$$

As initial conditions, each point has the following coordinates in the system of fixed coordinates X and Y:

$$\text{Point } A = \{0,0\}, \quad \text{Point } B = \{4,0\}, \quad \text{Point } C = \{0,0\}, \quad \text{Point } D = \{20,0\}$$

The initial velocity of the system is assumed to be zero.

The sequence of the mechanism is shown in Fig. 10. A first contact between point B and the beam N were observed at $t = 1.35$. After the first contact, the beam M was pushed back. Since the torque was applied continuously at point A, second contact was observed at $t = 2.05$. After the second contact, the beam M was pushed back once again. Since the bending rigidities were assumed to be small, large deformations were observed. This result shows the applicability of the meshless method into a flexible translational joint analysis.

7. Conclusions

The EFGM has been employed for an analysis of flexible translational joint. The modified shape function was proposed in which both ends of the element have the physical values. The reproducing condition or completeness of the modified shape functions was proved. The advantage of using the present shape function is that the essential boundary conditions are imposed by the same way as that of the FEM. Numerical examples show the applicability of the present method into a flexible multibody dynamic analysis.

References

Atluri, S.N., Zhu, T.-L., 1998. A new meshless local Petrov–Galerkin (MLPG) approach to nonlinear problems in computer modeling and simulation. Computer Modeling and Simulation in Engineering 3 (3), 187–196.

Belytschko, T., Lu, Y.Y., Gu, L., 1994. Element free Galerkin methods. Int. J. Numer. Methods Engrg 37, 229–256.
Belytschko, T., Krongauz, Y., Organ, D., Fleming, M., Krysl, P., 1996. Meshless methods: an overview and recent developments. Comput. Methods Appl. Mech. Engrg 139, 3–47.
Belytschko, T., Krongauz, Y., Dolbow, J., Gerlach, C., 1998. On the completeness of meshfree particle methods. Int. J. Numer. Methods Engrg 43, 785–819.
Cardona, A., Geradin, M., 1991. Modeling of superelements in mechanism analysis. Int. J. Numer. Methods Engrg 32 (8), 1565–1593.
Duarte, C.A., Oden, J.T., 1996. An h–p adaptive method using clouds. Comput. Methods Appl. Mech. Engrg 139, 237–262.
Escalona, J.L., Hussien, H.A., Shabana, A.A., 1998. Application of the absolute nodal coordinate formulation to multibody system dynamics. J. Sound Vib 214 (5), 833–851.
Gunther, F.C., Liu, W.K., 1998. Implementation of boundary conditions for meshless methods. Comput. Methods Appl. Mech. Engrg 163, 205–230.
Haug, E.J., 1989. Computer-Aided Kinematics and Dynamics of Mechanical Systems. Allyn and Bacon, Newton, MA.
Iura, M., Atluri, S.N., 1988. Dynamic analysis of finitely stretched and rotated three-dimensional space-curved beams. Computers and Structures 29 (5), 875–889.
Iura, M., Atluri, S.N., 1989. On a consistent theory, and variational formulation of finitely stretched and rotated 3D space-curved beams. Compt. Mech 4, 73–88.
Iura, M., Atluri, S.N., 1995. Dynamic analysis of planar flexible beams with finite rotations by using inertial and rotating frames. Computers and Structures 55 (3), 453–462.
Kaljevic, I., Saigal, S., 1997. An improved element free Galerkin formulation. Int. J. Numer. Methods Engrg 40, 2953–2974.
Krongauz, Y., Belytschko, T., 1996. Enforcement of essential boundary conditions in meshless approximations using finite elements. Comput. Methods Appl. Mech. Engrg 131, 133–145.
Lu, Y.Y., Belytschko, T., Gu, L., 1994. A new implementation of the element free Galerkin method. Comput. Methods Appl. Mech. Engrg 113, 397–414.
Liu, W.K., Jun, S., Li, S., Adee, J., Belytschko, T., 1995. Reproducing kernel particle methods for structural dynamics. Int. J. Numer. Methods Engrg 38, 1655–1679.
Melenk, J.M., Babuska, I., 1996. The partition of unity finite element methods: basic theory and applications. Comput. Methods Appl. Mech. Engrg 139, 289–314.
Modaressi, H., Aubert, P., 1996. A diffuse element-finite element technique for transient coupled analysis. Int. J. Numer. Methods Engrg 39, 3809–3838.
Nayroles, B., Touzot, G., Villon, P., 1992. Generalizing the finite element method: diffuse approximation and diffuse elements. Compt. Mech 10, 307–318.
Onate, E., Idelsohn, S., Zienkiewicz, O.C., Taylor, R.L., 1996. A finite point method in computational mechanics. Applications to convective transport and fluid flow. Int. J. Numer. Methods Engrg 39, 3839–3866.
Reissner, E., 1981. On finitely deformations of space-curved beams. J. Appl. Math. Phy. (ZAMP) 132, 734–744.
Simo, J.C., Vu-Quoc, L., 1986. On the dynamics of flexible beams under large overall motions — the plane case: Part 1 and Part 2. J. Appl. Mech., ASME 53, 849–863.